

Direct Observation of Dislocations in Potash Alum

By SAYEDA H. EMARA†, B. R. LAWN‡ and A. R. LANG
H. H. Wills Physics Laboratory, University of Bristol

[Received 16 August 1968]

ABSTRACT

X-ray topography shows that single-crystal octahedra of potash alum grown from solution may contain very few dislocations, most of them being generated in the initial stage of crystal growth. In crystals of irregular habit more dislocations are found outcropping on the faster-growing faces than on the slower. Some crystals are sufficiently perfect to permit absolute measurement of the x-ray structure factor from the the x-ray Pendellösung period.

THIS investigation of lattice imperfections in potash alum crystals was prompted by the findings of Omar and Youssef (1961) that a light etching of the octahedral faces of alum crystals produced shallow triangular pyramidal pits similar in shape and orientation to the pyramidal 'trigons' commonly present on natural diamond octahedral faces. A strong argument in favour of natural diamond trigons being etch pits, based on a study of trigon morphology, was put forward by Frank, Puttick and Wilks (1958). These authors also suggested that pyramidal trigons were situated at dislocation outcrops. Early x-ray topographic studies on diamond by Frank and Lang (1959) gave support to this idea, and further x-ray topographic work by Lang (1964) fully demonstrated the association of dislocation outcrops with the apices of pyramidal trigons. It was therefore of interest to discover whether potash alum crystals produced in a similar way to those studied by Omar and Youssef possessed dislocations in a configuration like that found in diamond, and in a number of the right order to be in accord with the trigon densities produced on the alum faces.

Potash alum crystals were prepared as follows. A small seed crystal was suspended in a saturated aqueous solution of pure potash alum at about 80°C which was then allowed to cool down to a steady room temperature of about 18°C. After 24 hours a well-developed octahedral crystal was formed by addition to the seed. Other crystals grew at the bottom of the containing vessel; these were generally tabular in habit. In some crystallization experiments, evaporation of solution was hastened by reducing pressure over it with a rotary vacuum pump. Specimens in the size range 2 to 5 mm, and having smooth faces free from overgrowths (as judged by examination in a metallurgical microscope) were selected for

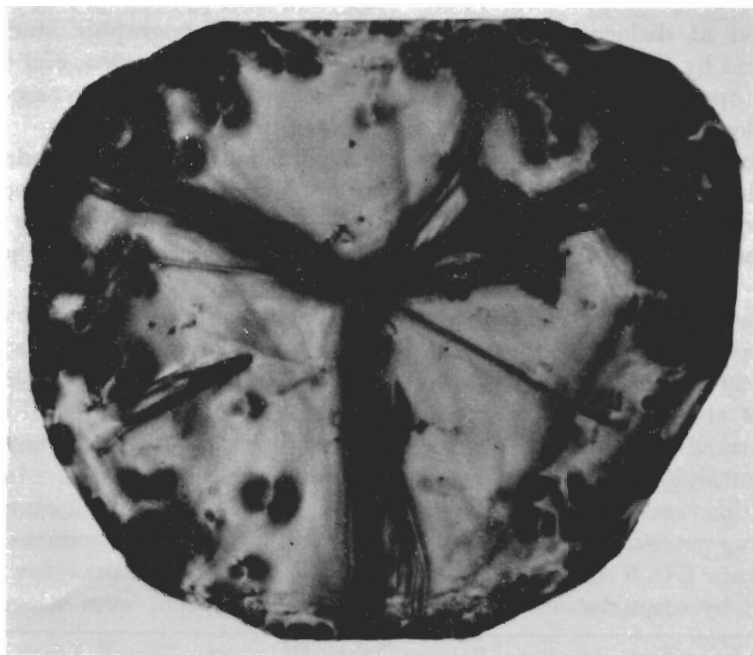
† On leave from Faculty of Science, Libya University, Tripoli, Libya.

‡ Now at School of Physics, University of N.S.W., Kensington, N.S.W., Australia.

x-ray topographic examination. The tabular crystals were especially convenient for study since the greater ratio of their (large) faces to the crystal thickness, compared with a regular octahedron, provided large-area topograph images with minimal confusion due to superimposition of images of lattice defects distributed within the thickness of the crystal, provided that the crystal was suitably oriented during examination. Favourable orientation was achieved in the x-ray projection topographs (Lang 1959) by using the strong 220 reflection from planes normal to the large pair of octahedral faces, and setting these faces perpendicular to the plane of incidence and diffraction. Since the Bragg angle was small ($3\frac{3}{4}^\circ$) for the radiation used (Ag $K\alpha_1$), the topographs give a view of the crystal looking almost normal to the large octahedral faces. Bearing this in mind, the shape of the topographs of the three tabular crystals shown in figs. 1 (a)–(c) may be understood. All topographs described here were taken with the reflection and radiation stated above. They are shown as positive prints of the original plates (i.e. greater blackness means greater diffracted intensity) and are oriented with the diffraction vector, \mathbf{g} , horizontal.

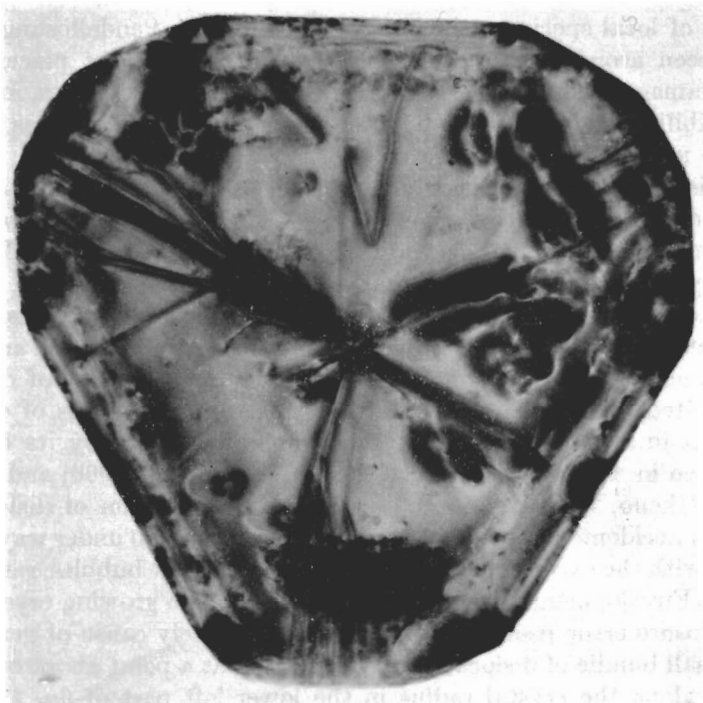
All crystals show intensification of diffracted intensity from localized surface damage: this is particularly severe at crystal corners. The large crystal whose topograph is shown in fig. 1 (c) has relatively undamaged

Fig. 1

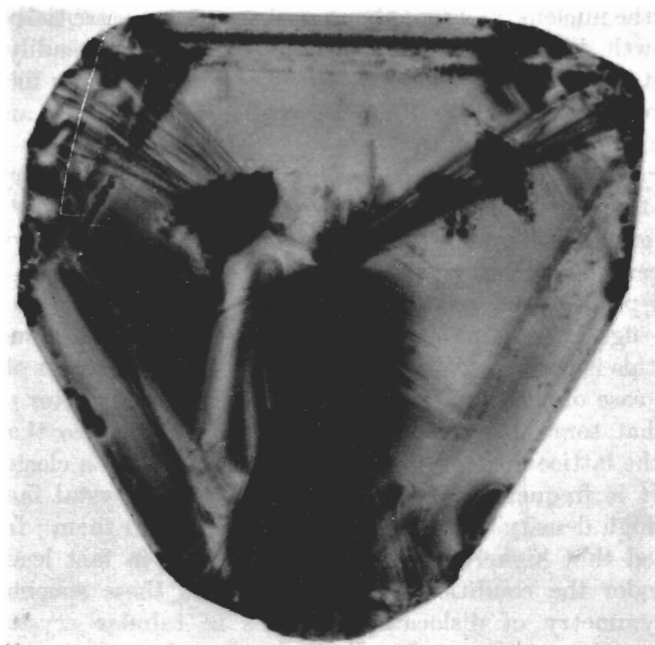


(a)

Fig. 1 (continued)



(b)



(c)

edges, and along the top edge of the image regular finely spaced Pendellösung fringes can be seen (Kato and Lang 1959) which correspond to contours of local specimen thickness. Less regular Pendellösung fringes can be seen around the margins of figs. 1 (a) and (b) at places where crystal damage is not severe. The appearance of these fringes, and their good visibility, show that the body of the crystal is behaving as perfect, from the x-ray diffraction point of view.

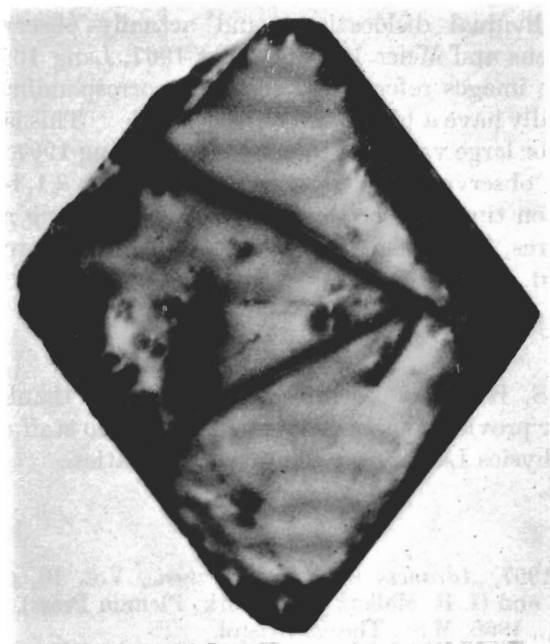
The dislocation configuration shown in figs. 1 (a)–(c), which consists of bundles of dislocations, or sometimes just single dislocations, radiating from a central nucleus and grown in to the crystal nearly perpendicularly to the crystal faces, is found in numerous alum specimens, both tabular and equiaxed. It is strongly reminiscent of the most common dislocation configuration in diamond (examples of this are shown in Frank and Lang (1965) in addition to those in the x-ray topographic studies of diamond already cited). Indeed it appears that this configuration is of common occurrence in crystals grown from solution, as evidenced by its frequent appearance in x-ray topographs of hexamine (Duckett 1966) and sodium chloride (Ikeno, Maruyama and Kato 1968). Generation of dislocations at growth accidents happening later, after growth is well under way, is rare in alum (with the exception of dislocation generation at bubbles, referred to below). Envelopment of a mote of impurity by the growing crystal, and lattice closure error resulting therefrom, is the likely cause of generation of the small bundle of dislocations seen starting at a point about one-third the way along the crystal radius in the lower left part of fig. 1 (a), and of the pair of dislocations that start some distance above the central nucleus in fig. 1 (b). The observation that the majority of dislocations start from the nucleus, and that their number is not substantially increased during growth, implies that the *density* of dislocations steadily decreases as the crystal gets larger. Thus in larger crystals one may find volumes in the range of several cubic millimetres quite dislocation-free, and diffracting as ideally perfect crystals.

Some crystals have bubbles distributed as strings along crystal radii normal to faces, or concentrated as veils roughly parallel to crystal faces at certain growth horizons. Veils occurring in the faster-growing sectors (i.e. between the nucleus and the smaller crystal faces) are sources of strain and produce patches of intense diffraction contrast on the topographs in figs. 1 (a)–(c). Often the bubbles generate numerous dislocations (this is well exemplified in the upper left-hand sector of fig. 1 (c)), but in the case of the bubbles in the upper right-hand sector of fig. 1 (a) it seems that some dislocations terminate on bubbles, so that in some instances the lattice heals to make a perfect crystal when closing round a bubble. It is frequently observed that the small crystal faces have a relatively high density of dislocations outcropping on them; from this it is concluded that higher dislocation density does in fact lead to faster growth, under the conditions of preparation of these specimens. The trigonal symmetry of dislocation bundles in tabular crystals, shown

especially well by fig. 1 (a), is a common feature of such crystals and is reflected in the relative development of their faces. The mechanism of nucleation which favours production of just three such dislocation bundles is unknown.

Figure 2 shows a small regular octahedron, oriented with a cube axis vertical. The front and back faces have largely escaped damage and fairly regular Pendellösung fringes appear in the double wedge formed between them. Assuming the angle between these faces to be that of a

Fig. 2



X-ray topograph of regular octahedron, edge length 1.6 mm.

perfect octahedron, $70\frac{1}{2}^\circ$, the x-ray extinction distance, ξ_g , can be easily computed from the fringe spacing on the topographs. The value derived is $198\ \mu\text{m}$ which is within a few per cent of the value of $207\ \mu\text{m}$ that corresponds to the 220 structure factor calculated by Lipson and Bevers (1935). A measurement from so few fringes cannot be expected to be precise, but it is a promising indicator that good, absolute structure factor measurements could be made on larger crystals. Strain causes some bending of the fringes in fig. 2 where they approach regions of surface damage. This suggests that the measured value of ξ_g may well be slightly smaller than that obtainable from a completely undistorted crystal since the general effect of strains is to contract the fringe spacing (Kato 1963, 1964, Kato and Ando 1966, Hart 1966).

The space group of alum is Pa3, so the expected Burgers vector, \mathbf{b} , is a cube edge, \mathbf{a} . In 220-type reflections on average one-third of all dislocations should have $\mathbf{g} \cdot \mathbf{b} = 0$ and hence be very weakly visible (or, under special conditions of dislocation line orientation be quite invisible (Howie and Whelan 1962)). Disregarding the possibility of total invisibility, it does appear that the crystal shown in fig. 2 contains only three (or possibly four) internal dislocations. The interpretation of the dislocation images in fig. 2 as being due to single dislocations (and, also, the single image extending to lower right of the nucleus in fig. 1 (a), together with images of similar width and density in other topographs) is based upon the agreement of the apparent image width with that predicted for individual dislocations, and actually observed in perfect crystals (Wilkins and Meier 1963, Authier 1967, Lang 1967). It will be noted that the images referred to above as corresponding to single dislocations actually have a bimodal intensity profile. This is both expected and observed for large values of ξ_g and/or $\mathbf{g} \cdot \mathbf{b}$ (Lang 1967, Authier 1967). In the present observations it is assumed that $\mathbf{g} \cdot \mathbf{b} = 1$, but ξ_g is in the range five to ten times larger than in the case of strong reflections from simple structures, upon which most x-ray topographic work to date has been performed.

ACKNOWLEDGMENTS

One of us, S. H. Emara, wishes to express her thanks to Professor F. C. Frank for providing laboratory facilities and to staff members of the H. H. Wills Physics Laboratory for their cooperation.

REFERENCES

- AUTHIER, A., 1967, *Advances in X-ray Analysis*, Vol. 10, edited by J. B. Newkirk and G. R. Mallett (New York: Plenum Press), p. 9.
- DUCKETT, R. A., 1966, M.Sc. Thesis, Bristol.
- FRANK, F. C., and LANG, A. R., 1959, *Phil. Mag.*, **4**, 383; 1965, *Physical Properties of Diamond*, edited by R. Berman (Oxford: Clarendon Press), Chap. III, p. 69.
- FRANK, F. C., PUTTICK, K. E., and WILKS, E. M., 1958, *Phil. Mag.*, **3**, 1262.
- HART, M., 1966, *Z. phys.*, **189**, 269.
- HOWIE, A., and WHELAN, M. J., 1962, *Proc. R. Soc. A*, **267**, 206.
- IKENO, S., MARUYAMA, H., and KATO, N., 1968, *Proceedings of International Conference on Crystal Growth*, Birmingham, to be published in *J. Crystal Growth*.
- KATO, N., 1963, *J. phys. Soc. Japan*, **18**, 1785; 1964, *Ibid.*, **19**, 67, 971.
- KATO, N., and ANDO, Y., 1966, *J. phys. Soc. Japan*, **21**, 964.
- KATO, N., and LANG, A. R., 1959, *Acta crystallogr.*, **12**, 787.
- LANG, A. R., 1959, *Acta crystallogr.*, **12**, 249; 1964, *Proc. R. Soc. A*, **278**, 234; 1967, *Advances in X-ray Analysis*, Vol. 10, edited by J. B. Newkirk and G. R. Mallett (New York: Plenum Press), p. 91.
- LIPSON, H., and BEEVERS, C. A., 1935, *Proc. R. Soc. A*, **148**, 664.
- OMAR, M., and YOUSSEF, T. H., 1961, *Phil. Mag.*, **6**, 791.
- WILKENS, M., and MEIER, F., 1963, *Z. Naturf. A*, **18**, 26.